

Trioctylphosphine as Both Solvent and Stabilizer to Synthesize CdS Nanorods

Shutang Chen · Xiaoling Zhang · Qiuhua Zhang ·
Weihong Tan

Received: 21 March 2009 / Accepted: 4 June 2009 / Published online: 17 June 2009
© to the authors 2009

Abstract High quality CdS nanorods are synthesized reproducibly with cadmium acetate and sulfur as precursors in trioctylphosphine solution. The morphology, crystalline form and phase composition of CdS nanorods are characterized by transmission electron microscopy (TEM), high-resolution TEM and X-ray diffraction (XRD). CdS nanorods obtained are uniform with an aspect ratio of about 5:1 and in a wurtzite structure. The influence of reaction conditions on the growth of CdS nanorods demonstrates that low precursor concentration and high reaction temperature (260 °C) are favorable for the formation of uniform CdS nanorods with 85.3% of product yield.

Keywords CdS nanorods · Trioctylphosphine · Size control · Photoluminescence

Introduction

Nanoscale one-dimensional semiconductor materials have drawn much attention due to their unique mechanical, optical, and electronic properties [1–3]. Among metal

chalcogenides, cadmium sulfide is of particular interest because of its intrinsic direct band gap (2.5 eV), which has shown great potentials in bioimaging [4], solar energy conversion [5, 6] and photocatalysis [7]. During the past few years, much effort has been devoted to the development of synthetic approaches for one-dimensional CdS nanomaterials. Various methods, such as anodic aluminum oxide (AAO) template-assisted synthesis [8], hydrothermal process [9], solution–liquid–solid (SLS)-assisted growth [10, 11], seeded-type growth [12], colloidal micellar [13, 14] and single-source molecular precursor route [15, 16] have been developed and extensively studied. However, harsh conditions, complicated reagents, usage of sacrificial templates or guiding catalysts are required in these processes, which may complicate the application of the nanostructures. Very recently, the synthesis of CdS nanorods has been achieved via thermal decomposition of two precursors in a mixture of binary surfactants [17–20]. However, all these synthetic schemes require delicate control of amount of alkylphosphonates or surfactant ratios. Until now, the monosurfactant can be used for the formation of CdS nanorods [15, 16, 21]. Although, many methods have been reported for synthesis of colloidal CdS nanorods, only Yong et al. [21] reported the successful synthesis of CdS nanorods using a hot colloidal method, starting with oleylamine as the single surfactant. Non-catalytic and alkylphosphonates-free, solution-based synthesis methods are more effective for low-cost and large volume production than other methods for synthesizing colloidal nanorods. In this paper, we describe a new synthesis that favors growth of CdS nanorods under nonextreme conditions. Only tri-*n*-octylphosphine (TOP) both as solvent and stabilizer was required for the synthesis. The method is simple and suitable for the large-scale preparation of high-quality CdS nanorods.

S. Chen · X. Zhang (✉) · Q. Zhang
Department of Chemistry, School of Science, Beijing Institute of Technology, 100081 Beijing, People's Republic of China
e-mail: zhangxl@bit.edu.cn

W. Tan
Center for Research at the Bio/Nano Interface, University of Florida, Gainesville, FL 32611-7200, USA
e-mail: tan@chem.ufl.edu

Materials and Methods

Materials

TOP (90%) was purchased from Alfa Aesar Chemicals and used without further purification. Sulfur powder, $\text{Cd}(\text{CH}_3\text{CH}_2\text{COO})_2 \cdot 2\text{H}_2\text{O}$ and solvents used were purchased from Beijing Chemical Reagents Co.

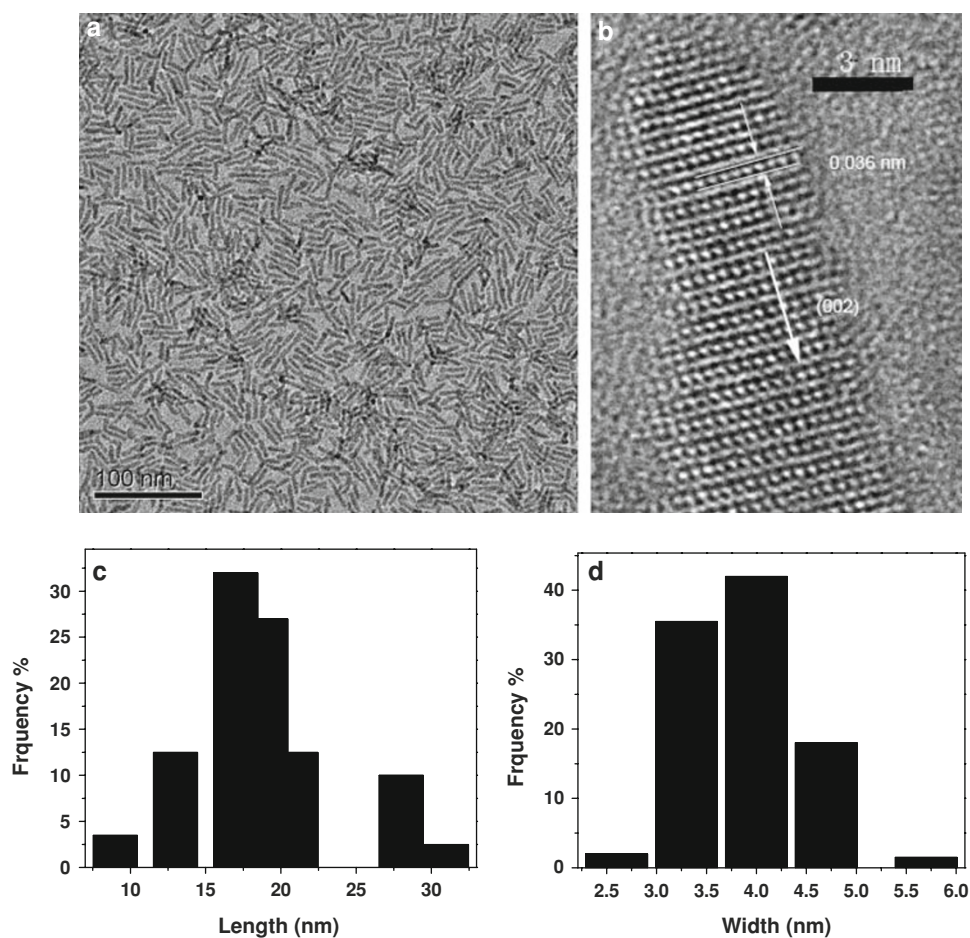
Synthesis of CdS Nanorods

In brief, cadmium acetate (40 mg) was first dissolved in 3 mL hot TOP under N_2 flow. Separately, elemental sulfur powder (24.0 mg) was added to TOP (1 mL) and mixed vigorously until dissolved. Next, the sulfur solution was injected to the cadmium solution and mixed thoroughly at 260 °C. The resulting yellow solution was stirred at 260 °C for reaction 6 h, cooled to 50 °C and finally methanol was added to give a fine deposit of CdS nanorods, which was separated by centrifugation and dissolved in toluene. The above centrifugation and isolation procedure was then repeated several times for purification of the CdS nanorods.

Characterization of CdS Nanorods

The size and shape of these CdS nanorods were examined using transmission electron microscopy (TEM) and high resolution TEM (HRTEM). TEM and electron diffraction (ED) were obtained with Jeol-200CX (operated at 120 kV), and HRTEM image was obtained with FET TECNAI F30 (operating at 300 kV), respectively. The sample for TEM was prepared by placing a drop of toluene dispersion of nanorods on the amorphous carbon-coated copper grids. The structure of the nanorods was investigated by X-ray diffraction (XRD) using a Rigaku D/MAX 2400 X-ray diffractometer with Cu K_α radiation ($\lambda = 1.5405 \text{ \AA}$). Prior to the XRD measurements, the samples were prepared by spreading several drops of CdS nanorods on the glass substrate. The surface of CdS nanorods was measured by using a VG ESCALAB-5 X-ray photoelectron spectrometry (XPS) system. Optical absorption spectra were collected at room temperature on a PE Lambda 35 Ultraviolet-visible (UV-Vis) spectrometer using 1-cm quartz cuvettes. The toluene solvent was used for the background sample. Room temperature photoluminescence (PL) measurement was

Fig. 1 CdS nanorods synthesized in TOP solution (40 mg cadmium acetate in 3 mL TOP and 24 mg S powder in 1 mL TOP at 260 °C for reaction 4 h): TEM image (a), HRTEM image (b), length (c) and width (d) distribution histograms of the nanorods



carried out on a SPEX Fluorolog-2 spectrometer of front face collection with 500- μm slits. PL spectra were collected between 400 and 700 nm at room temperature with 360 nm excitation powers. The Fourier-transform infrared spectra (FTIR) of the samples were recorded using a Bruker Equinox 55.

Results and Discussion

The morphology and dimension of the product were examined by TEM and HRTEM. Figure 1a shows the morphology of the CdS sample with 85.3% of product yield obtained after heating at 260 °C for reaction 4 h. The size distributions were evaluated by measuring the length and width of more than one hundred nanorods randomly selected from the TEM images. The length and width distributions of the CdS nanorods are shown in Fig 1c,d. The aspect ratio of the nanorods is about 5:1. It can be seen that the product is composed of uniform nanorods with an average width of 3.8 nm ($\sigma = 3\%$) and

length of 18.7 nm ($\sigma = 25\%$). Figure 1b shows an HRTEM image of an individual CdS nanorod. The clear crystal lattice fringes demonstrate that the nanorod is well crystallized. Furthermore, the HRTEM image reveals that the interplanar distance along the growth axis is 0.336 nm, which is consistent with the interplanar distance of the (002) plane of the wurtzite structure of CdS, thus confirming that the nanorods are elongated along the c axis.

Figure 2a shows the XRD patterns of the as synthesized CdS nanorods under the same conditions for reaction 2, 4 and 6 h, respectively. The CdS diffraction patterns show obviously broad peaks because smaller size of CdS nanocrystals was formed. The structure based on the XRD pattern is consistent with predominantly the hexagonal phase. The (100), (002), (101), (102), (110), (103) and (112) planes of wurtzite CdS are clearly distinguishable in the pattern (JCPDS 41-1049). From the XRD pattern, the relative intensity of the (002) peak increases with the prolonging of reaction time, which indicates the crystals are grown along the c -axis. The ED pattern (shown in Fig. 2b) consists of broad diffuse rings, further confirming

Fig. 2 Powder X-ray diffraction patterns **a** of CdS nanorods prepared with different reaction times while all other conditions kept the same (40 mg cadmium acetate in 3 mL TOP and 24 mg S powder in 1 mL TOP at 260°) for (a) 2 h, (b) 4 h and (c) 6 h, respectively; **b** ED patterns of CdS nanorods obtained at 260 °C for 4 h

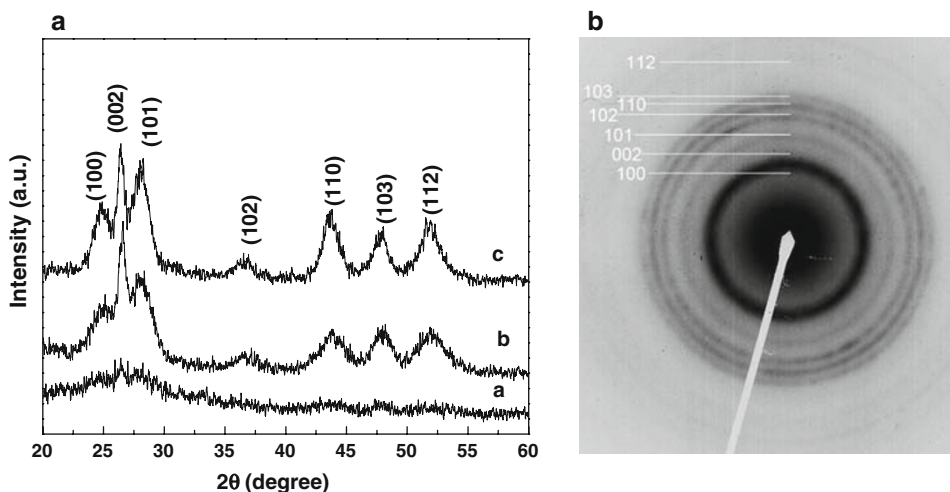
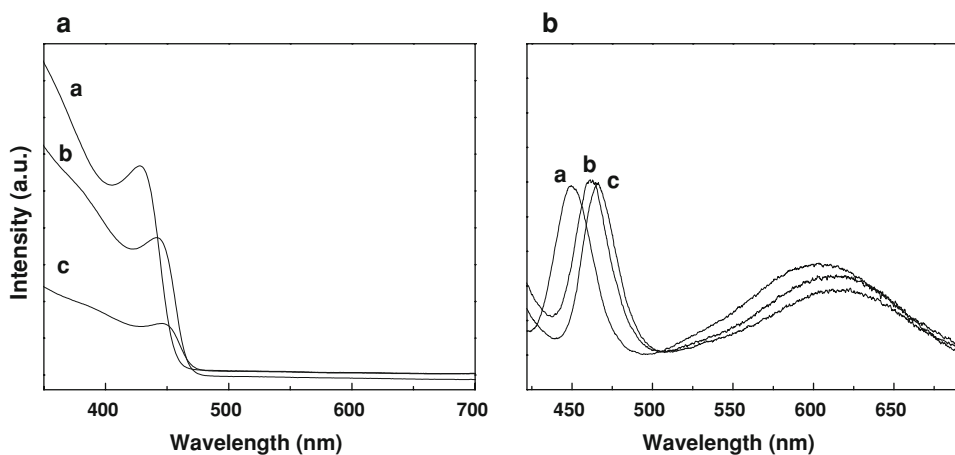


Fig. 3 Normalized optical absorption (a) and photoluminescence (b) spectra of CdS nanorods prepared with different reaction times while all other conditions kept the same (40 mg cadmium acetate in 3 mL TOP and 24 mg S powder in 1 mL TOP at 260 °C) for reaction (a) 1 h, (b) 2 h and (c) 4 h, respectively



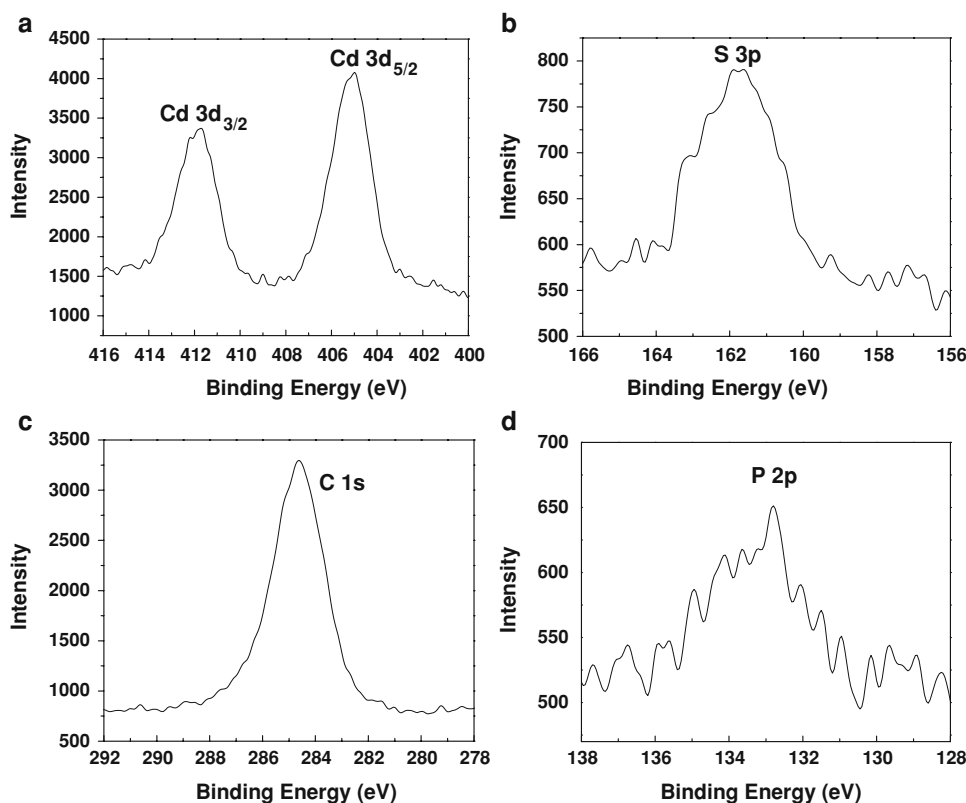
the crystalline nature of the CdS nanorods. The diffraction rings can be indexed to (100), (002), (101), (102), (110), (103) and (112) planes. This is consistent with the result of XRD.

Figure 3 shows the UV–Vis absorption (A) and PL (B) spectra of the as-synthesized CdS nanorods for different reaction times. From the absorption spectrum (Fig. 3a), it can be seen that the excitonic absorption peaks are well defined with a maximum at about 428, 442 and 450 nm, respectively. It is already known that the excitonic absorption peak is associated with the lowest optical transition and it provides a simple way to determine the nanocrystal bandgap. For the CdS nanorods, the absorption peak is 428, 442 and 450 nm, corresponding to bandgap of 2.89, 2.80 and 2.75 eV. A comparison with the value of bulk CdS (2.42 eV) [22] shows that the band edge is blueshifted, indicating the quantum size effect of the CdS nanorods. Figure 3b shows the PL spectra of the CdS nanorods with two emission peaks. The PL spectrum is redshifted compared to the absorption spectrum, which indicated the large Stokes shift of the nanorods. The appearance of the first exciton peak around 455 nm indicates that there is a control of the size distribution in the transverse direction. Thus, the corresponding luminescence peak around 455 nm originates from the band edge of the as-prepared CdS nanorods. In addition to the excitonic

emission, the broad band emission from 508 nm extended to the region of near infrared arises from the defect states of CdS nanocrystals. Notably, the ratio of emission intensity for the defect emission (508 nm) versus band-edge emission (455 nm) decreases as the reaction time increasing, evidently representing CdS nanorods with fewer defects may be prepared after reaction for 4 h.

The chemical compositions of the sample were studied by XPS shown in Fig. 4. The S 2p, Cd 3d_{5/2} and Cd 3d_{3/2} peaks in the spectrum indicate that the composition of the final product consists of cadmium and sulfur elements. Although the amounts of phosphorus and carbon is small, the intense C 1s and P 2p peak are also observed in Fig. 4c, d, indicating the TOP molecules' binding to Cd on the nanocrystals surface. In order to clarify the source of the C and P element, FT-IR of the as-synthesized CdS nanorods and TOP were recorded as shown in Fig. 5. The FT-IR spectrum of TOP-stabilized CdS nanorods revealed the CH₂ stretching of TOP at 2,929 and 2,876 cm⁻¹, indicating that the TOP remains in its original form after the washing procedure. In the FT-IR spectrum of the CdS/TOP core/shell nanorods, the C–P stretching peaks of TOP appeared at 1,170, 1,076 and 1,032 cm⁻¹. The peak at 728 cm⁻¹ related with (–CH₂)_n (n ≥ 4) stretching of TOP was also observed. Moreover, the peak at 1,494, 1,456 and 1,381 cm⁻¹ originate from the asymmetric in-plane and

Fig. 4 XPS spectra of CdS nanorods prepared (40 mg cadmium acetate in 3 mL TOP and 24 mg S powder in 1 mL TOP at 260 °C for reaction 4 h) in TOP solution: **a** Cd; **b** S; **c** C; **d** P



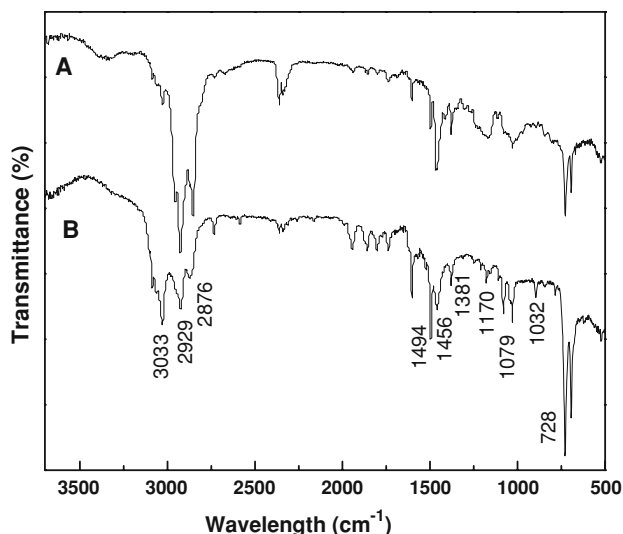


Fig. 5 FT-IR spectra of (a) pure TOP and (b) CdS/TOP core/shell nanorods

symmetric rocking mode of terminal methyl group of TOP. From these data, it could be confirmed that the TOP was successfully capped on the CdS surface.

Fig. 6 TEM images of CdS nanorods obtained with different reaction times while all other conditions kept the same (40 mg cadmium acetate in 3 mL TOP and 24 mg S powder in 1 mL TOP at 260 °C) for a 2 h, and b 6 h

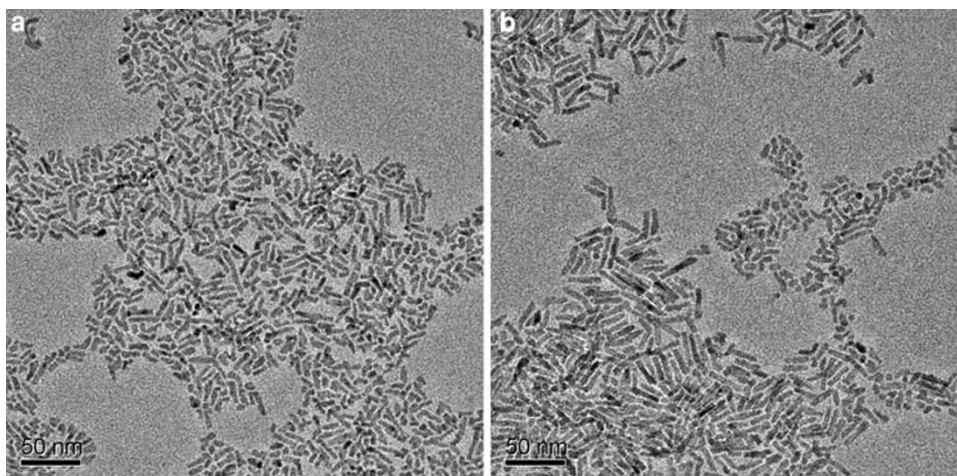
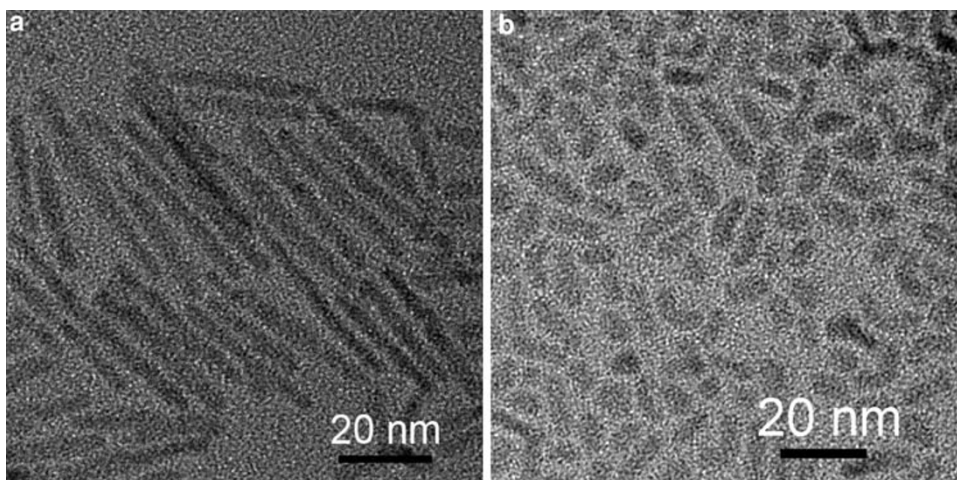


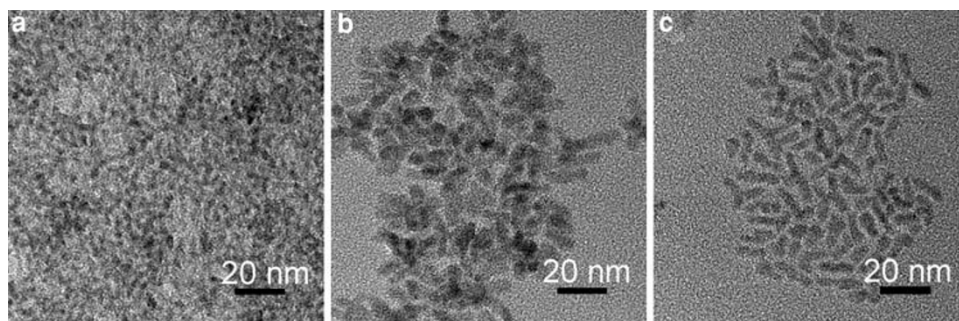
Fig. 7 TEM images of CdS samples synthesized at different precursor concentrations at 260 °C for reaction 4 h: a 20 mg cadmium acetate precursor in 3 mL TOP and 12 mg S powder dissolved in 1 mL TOP; b 80 mg cadmium acetate precursor in 3 mL TOP and 48 mg S powder dissolved in 1 mL TOP



In order to investigate the effect of the reaction conditions on the growth of CdS nanorods, we have systematically studied the growth of CdS nanorods by varying the reaction time, the precursor concentration and growth temperature. Figure 6 shows TEM images of the products prepared with different reaction times while all other conditions kept the same (40 mg cadmium acetate in 3 mL TOP and 24 mg S powder in 1 mL TOP at 260 °C). The length of CdS nanorods increases quickly just after injection S precursor. At the early of the reaction (2 h), short nanorods (about 10 nm in length) can be generated as shown in Fig. 6a. With reaction prolonging to 4 h, uniform CdS nanorods can be prepared (Fig. 1a). However, when the reaction time was extended to 6 h, the products became a mixture of nanorods (80%) and nanoparticles (20%) as shown in Fig. 6b. As the monomer concentration depletes during growth, the aspect ratio gradually decreases to nearly one (ordinary quantum dots). Thus, size-controlled CdS nanorods can be synthesized by tuning reaction time.

Another important factor that controls the length of nanorod is the concentration of the Cd and Se precursor. In the sequence of samples shown in Fig. 7, the amount of

Fig. 8 TEM images of CdS nanorods synthesized at different reaction temperatures of **a** 180 °C, **b** 230 °C, and **c** 290 °C, while all other conditions kept the same (40 mg cadmium acetate in 3 mL TOP and 24 mg S powder in 1 mL TOP)



TOP is held fixed, and the total elapsed time is constant (4 h), while the precursor concentration is increased gradually. As the precursor concentrations are 20 mg cadmium acetate in 3 mL TOP and 12 mg S powder in 1 mL TOP, long nanorods (about 45 nm) are obtained as shown in Fig. 7a. It can be seen from Fig. 7a that the nanorods are not uniform, compared with that prepared from 40 mg cadmium acetate in 3 mL TOP and 24 mg S powder in 1 mL TOP (Fig. 1a). When the concentration is four times as that for the long CdS nanorods were formed, the products are mainly short nanorods with a few nanoparticles (Fig. 7b). The average length of nanorod increases significantly as the precursor concentration is decreased. These observations can be explained if the overall growth process is considered to occur in two steps: the initial formation of nuclei just after supersaturation and the subsequent process of growth of nuclei [20, 23, 24]. At low concentration of precursors, relatively few nuclei form, so that the available amount of monomer per nucleus during the growth phase is relatively high. This leads to a fast growth and more long nanorod (which is dynamically favored). Under high concentration of precursors, many nuclei form so that the available monomer per nucleus during the growth phase is relatively low. This leads to slower growth and shorter nanorods.

For the study of the effect of reaction temperature on CdS nanorod formation, CdS samples were prepared with heating for 4 h. As can be seen TEM images from Fig. 8, at 180 °C, close to quasi-nanorods are obtained. When the reaction temperature was increased to 230 °C, aggregated short nanorods can be observed (Fig. 8b). Irregular short nanorods became the most possible product under 290 °C (Fig. 8c). Finally, attempts have also been made to further increase the temperature above 320 °C to grow CdS nanorods. However, the results of TEM and UV–Vis analysis (not shown here) indicated that few CdS nanorod were formed. We tentatively attribute the phenomena to the possibility that above 320 °C the mixture becomes an azeotrope, as evidenced by the boiling of the colorless solution, the turbulence from which might disturb the growth of CdS crystals [18]. These observations show that the reaction temperature also significantly affects the

morphology of the CdS nanocrystals. It can be reasonably concluded that low precursor concentration and high reaction temperature are favorable for the formation of CdS nanorods. At 260 °C for reacting for 4 h, uniform CdS nanorods are generated as shown in Fig. 1a.

Conclusion

In conclusion, we have demonstrated the formation of CdS nanorods by using TOP as single-coordinating solvent. It is worth mentioning that the growth conditions are simple and also can be easily adopted for large-scale preparations. Also, no additional solvents and stabilizers are needed. This process may bring conveniences to explore the capping mechanism of nanocrystallites surface. Attempts to grow other II–VI semiconductor nanorods with the present synthesis scheme are being pursued. Theoretical calculations are also underway to gain an insight into the mechanism of rod formation.

Acknowledgments The work is supported by the 111 Project B07012. The authors would like to express our sincere thanks to Prof. H J Gao and C M Shen from Institute of Physics (Chinese Academy of Sciences) for their assistance in the experiments and helpful discussions.

References

1. X.G. Peng, L. Manna, W.D. Yang, J. Wickham, E. Scher, A. Kadavanich, A.P. Alivisatos, *Nature* **404**, 59 (2000). doi: [10.1038/35003535](https://doi.org/10.1038/35003535)
2. D.V. Talapin, A. Koeppel, S. Gotzinger, A. Kornowski, J.M. Lupton, A.L. Rogach, O. Benson, J. Feldmann, H. Weller, *Nano Lett.* **3**, 1677 (2003). doi: [10.1021/nl034815s](https://doi.org/10.1021/nl034815s)
3. S.J. Kim, C.S. Ah, D.J. Jang, *Adv. Mater.* **19**, 1064 (2007). doi: [10.1002/adma.200601646](https://doi.org/10.1002/adma.200601646)
4. S. Santra, H. Yang, P.H. Holloway, J.T. Stanley, R.A. Mericle, *J. Am. Chem. Soc.* **127**, 1656 (2005). doi: [10.1021/ja0464140](https://doi.org/10.1021/ja0464140)
5. N. Romeo, A. Bosio, V. Canevari, A. Podestà, *Sol. Energy* **77**, 795 (2004). doi: [10.1016/j.solener.2004.05.011](https://doi.org/10.1016/j.solener.2004.05.011)
6. J.B. Baxter, A.M. Walker, K.V. Ommering, E.S. Aydil, *Nanotechnology* **17**, S304 (2006). doi: [10.1088/0957-4484/17/11/s13](https://doi.org/10.1088/0957-4484/17/11/s13)
7. H. Fujii, M. Ohtaki, K. Eguchi, H. Arai, *J. Mol. A. Catal: Chem.* **129**, 61 (1998). doi: [10.1016/S0040-4039\(98\)01235-0](https://doi.org/10.1016/S0040-4039(98)01235-0)

8. D. Xu, D. Chen, Y. Xu, X. Shi, G. Guo, L. Gui, T. Tang, *Pure. Appl. Chem.* **72**, 127 (2000). doi:[10.1351/pac200678030633](https://doi.org/10.1351/pac200678030633)
9. R. Thiruvengadathan, O. Regev, *Chem. Mater.* **17**, 3281 (2005). doi:[10.1021/cm0500408](https://doi.org/10.1021/cm0500408)
10. T.J. Trentler, K.H. Hickman, S.C. Goel, A.M. Viano, P.C. Gibbons, W.E. Buhro, *Science* **270**, 1791 (1995). doi:[10.1126/science.1058120](https://doi.org/10.1126/science.1058120)
11. F. Wang, A. Dong, J. Sun, R. Tang, H. Yu, W.E. Buhro, *Inorg. Chem.* **45**, 7511 (2006). doi:[10.1021/ic060498r](https://doi.org/10.1021/ic060498r)
12. S.E. Habas, P.D. Yang, T. Mokari, *J. Am. Chem. Soc.* **130**, 3294 (2008). doi:[10.1021/ja800104w](https://doi.org/10.1021/ja800104w)
13. Y.W. Wang, G.W. Meng, L.D. Zhang, C.H. Liang, J. Zhang, *Chem. Mater.* **14**, 1773 (2002). doi:[10.1021/cm0115564](https://doi.org/10.1021/cm0115564)
14. C.C. Chen, C.Y. Chao, C.H. Lang, *Chem. Mater.* **12**, 1516 (2000). doi:[10.1021/cm981136n](https://doi.org/10.1021/cm981136n)
15. P.S. Nair, T. Radhakrishnan, N. Revaprasadu, G.A. Kolawole, P. O'Brien, *Chem. Commun.*, 564 (2002). doi:[10.1039/b200434h](https://doi.org/10.1039/b200434h)
16. Y.W. Jun, S.M. Lee, N.J. Kang, J.W. Cheon, *J. Am. Chem. Soc.* **123**, 5150 (2001). doi:[10.1021/ja0157595](https://doi.org/10.1021/ja0157595)
17. P. Christian, P. O'Brien, *Chem. Commun.* 2817 (2005). doi:[10.1039/b502711j](https://doi.org/10.1039/b502711j)
18. C.C. Kang, C.W. Lai, H.C. Peng, J.J. Shyue, P.T. Chou, *Small* **3**, 1882 (2007). doi:[10.1002/sml.200700390](https://doi.org/10.1002/sml.200700390)
19. A.E. Saunders, A. Ghezelbash, P. Sood, B.A. Korgel, *Langmuir*. **24**, 9043 (2008). doi:[10.1021/la800964s](https://doi.org/10.1021/la800964s)
20. Z.A. Peng, X.G. Peng, *J. Am. Chem. Soc.* **123**, 1389 (2001). doi:[10.1021/ja0027766](https://doi.org/10.1021/ja0027766)
21. K.T. Yong, Y. Sahoo, M.T. Swihart, P.N. Prasad, *J. Phys. Chem. C*. **111**, 2447 (2007). doi:[10.1021/jp066392z](https://doi.org/10.1021/jp066392z)
22. C.B. Murray, D.J. Norris, M.G. Bawendi, *J. Am. Chem. Soc.* **115**, 8706 (1993). doi:[10.1021/ja00072a025](https://doi.org/10.1021/ja00072a025)
23. S. Kumar, T. Nann, *Small* **3**, 316 (2007). doi:[10.1002/sml.200600425](https://doi.org/10.1002/sml.200600425)
24. C.R. Bullen, P. Mulvaney, *Nano. Lett.* **4**, 2303 (2004). doi:[10.1021/nl0496724](https://doi.org/10.1021/nl0496724)